ELSEVIER

International Journal of Mass Spectrometry 223–224 (2003) 67–79

International Journal of Mass Spectrometry

www.elsevier.com/locate/ijms

A photoionization mass spectrometric study of acetylene and ethylene in the VUV spectral region

R.A. Mackie, S.W.J. Scully, A.M. Sands, R. Browning, K.F. Dunn, C.J. Latimer*

Department of Pure and Applied Physics, The Queen's University of Belfast, Belfast BT7 1NN, UK

Received 20 December 2001; accepted 22 February 2002

Abstract

The molecular and dissociative photoionization of C_2H_2 and C_2H_4 has been studied using synchrotron radiation within the energy range 11–30 eV. Positive and negative photoion mass spectra have been obtained. Appearance thresholds for the formation of fragment ions have been determined and are compared with the thermochemical values. Above threshold it is shown that superexcited states, involving intravalence transitions and shape resonances which can decay through ion pair formation, play an important role in the photodissociative ionization process. The positive photoion yield curves display significant hitherto unobserved structures, which are unrelated to those present in the photoelectron spectra. (Int J Mass Spectrom 223–224 (2003) 67–79)

Keywords: Photoionization; Acetylene; Ethylene

1. Introduction

Acetylene (ethyne) C_2H_2 and ethylene (ethene) C_2H_4 are the prototype alkyne and alkene molecules, respectively. Numerous experimental and theoretical studies have been undertaken in an attempt to understand their bond energies and the excited neutral and ionic states that can be formed through photoabsorption in the VUV spectral region. Despite this, many important features of even the most basic processes involving these molecules are still not completely understood. In addition to being of fundamental interest, they are of considerable practical relevance. They play an important role in our understanding of the physics and chemistry of atmospheres and of the interstellar medium. They are increasingly used in dilute plasmas in the processing and fabrication of materials, including diamond films, while as hydrocarbon impurities they play a significant role in fusion plasma devices ([1,2] and references therein).

The photoelectron spectra arising from excitation of the inner and outer valence electrons have been investigated by many workers ([3–5] and references therein). In contrast, there have been relatively few investigations involving photoionization mass spectrometry. Brion and coworkers [6,7] have determined the absolute partial photoionization oscillator strengths for the molecular and dissociative photoionization channels in both C_2H_2 and C_2H_4 using low resolution dipole electron impact (e, e + ion) coincidence

* Corresponding author. E-mail: c.latimer@qub.ac.uk

1387-3806/02/$ – see front matter
PII S1387-3806(02)00781-9

spectroscopy ($\Delta E \sim 1$ eV) at equivalent photon energies from threshold to 80 eV.

Photoionization efficiency curves for the production of $C_2H_2^+$ and C_2H^+ ions in acetylene at photon energies up to 20 eV have been studied by Botter et al. [8] and Berkowitz [9]. More recently, Hayaishi et al. [10] have performed a more comprehensive study, in which the formation of the molecular ion and the carbon containing molecular fragment ions have been studied within the energy range 11–30 eV. In all these studies, substantial structure, due to autoionizing states which are still not fully identified and assigned, has been observed in the formation of the $C_2H_2^+$ ion in the energy region 11–18 eV, which encompasses the ground and first excited state of the ion. Above this region higher excited states and additional superexcited states, which have several different decay channels, including dissociative autoionization, can play an important—and often dominant—role in the absorption process.

In the case of ethylene, photoionization efficiency curves for the formation of $C_2H_4^+$ and the $C_2H_3^+$ and $C_2H_2^+$ fragment ions below 16.5 eV have been measured in earlier work by Botter et al. [8] and Chupka et al. [11] using conventional light sources. In contrast to the situation in acetylene, no autoionization effects are seen between the ground and first excited state of the parent ion. Stockbauer and Inghram [12] have discussed the importance of eliminating autoionization effects in experimental tests of quasi-equilibrium theory (QET). In such experiments, at energies up to 19 eV, they have shown that the decomposition of $C_2H_4^+$ provides "a textbook example of the success of QET" [9]. In an investigation limited to the observation of the photoionization efficiency curve of the parent molecular ion, Wood and Taylor [13] have observed features which they consider to correspond to seven autoionizing Rydberg states above the first excited state of the parent ion, in the energy region 12.1–16.5 eV, implying that the resultant ion states decay statistically. It is worth noting that such statistical decay precludes the acquisition of any information concerning those states initially excited, as these transfer by radiationless transitions to the electronic ground state (internal conversion, the basic mechanism of QET), which then determines the fragmentation process. However, as pointed out by Berkowitz [14], if QET is perfectly obeyed, ion pair formation should not occur. Thus, ion pair formation may be used [15,16] as a sensitive method of investigating the spectra and decay dynamics of superexcited states lying in the VUV.

In the present work, we have performed the most comprehensive study to date on the photoionization mass spectra of both acetylene and ethylene within the inner and outer valence energy range (11–30 eV), at an energy resolution of approximately 10 meV. For the first time negative photoion yield curves have also been measured over this energy range. Appearance potentials for the formation of all the fragment ions have been determined and compared with their thermochemical thresholds.

2. Experimental approach

The experiments were carried out at the Daresbury Laboratory UK Synchrotron Radiation Source on beamline 3.2, using experimental arrangements and procedures almost identical to those described in our earlier work on the dissociative photoionization of hydrogen and methane gases [17]. Experiments were performed within the photon energy range 12–35 eV using a normal incidence McPherson 5m monochromator, which provided a flux of approximately 10^{11} $h\nu$/s with a bandpass of 1 Å, was horizontally polarized (>40%) and contained <5% second order radiation. The photon beam emerged from a capillary light guide, was crossed at 90° by a low pressure gas jet of either acetylene or ethylene, and detected using an aluminium photocathode. The photon flux was obtained by taking into account the relative detection efficiency of the photocathode with photon wavelength [18]. The positive or negative ions formed were extracted from the interaction region with an electric field and injected into a triple–quadrupole mass spectrometer (Hiden Analytical HAL IV), mounted in a differentially pumped chamber, for analysis and detection. In

such a set up it is notoriously difficult to avoid mass discrimination effects due to the quadrupole filter ion detector response and loss of fragment ions which have substantial kinetic energy. In the present system, however, these effects were shown to be negligible in a subsidiary keV ion beam experiment involving a methane target, which gave results in good accord with well-established proton impact data known to be free from such problems [19]. In addition, our recent studies on the photoionization mass spectra of ethane are in satisfactory agreement with earlier work known to be free from such effects [16].

3. Results and discussion

3.1. Acetylene

The acetylene molecule has a linear $D_{\infty h}$ geometry and the ground state configuration and term [5]

$$\underset{\text{core orbitals}}{(1\sigma_g)^2(1\sigma_u)^2} \quad \underset{\text{inner valence}}{(2\sigma_g)^2(2\sigma_u)^2} \quad \underset{\text{outer valence}}{(3\sigma_g)^2(1\pi_u)^4} \quad {}^1\Sigma_g{}^+$$

with the four lowest lying virtual orbitals being $(1\pi_g)$, $(3\sigma_{lu})$, $(4\sigma_g)$ and $(4\sigma_u)$. High resolution HeI photoelectron spectroscopy has shown that the adiabatic ionization energies for $C_2H_2{}^+$ $X^2\Pi_u$, $A^2\Sigma_g{}^+$ and $B^2\Sigma_u{}^+$ states are 11.403, 16.297 and 18.391 eV, respectively and that ionization is well described by the independent particle model [5,20]. Following Holland et al. [5], we have retained the traditional notation $A^2\Sigma_g{}^+$ for the first excited state, to facilitate comparison with the results of previous workers.

The outer valence orbitals are based on C 2p and H 1s atomic orbitals and the inner valence mainly on C 2s and H 1s orbitals. For ionization from the inner valence $(2\sigma_g)$ orbital, the single particle model no longer holds and the photoelectron spectrum shows several satellite lines at energies above the main $C^2\Sigma_g{}^+$ line at 23.5 eV [5].

Photoion yield curves for the parent and main fragment ions formed in C_2H_2, taken with a resolution of 10 meV, are shown in Figs. 1 and 2, along with the photoelectron spectrum of Holland et al. [5] recorded at a photon energy of 110 eV. The $C_2H_2{}^+$ ions were also observed, but typically contribute less than 0.3% to the total ionization in this energy range. Where comparison is possible, the general features of present data are in satisfactory accord with earlier experimental work [1].

The photoion yield curve for the parent $C_2H_2{}^+$ ion is shown in more detail in Fig. 3. The appearance energy of 11.40 ± 0.05 eV is in excellent accord with the value established by photoelectron spectroscopy. In the region up to 2 eV above threshold substantial structure is seen, which has been well detailed in earlier ion yield work and assigned to autoionizing Rydberg series converging to vibrationally excited levels of the electronic ground state. At higher energies, a number of prominent features are observed which have also been seen in photoabsorption [21] and threshold photoelectron spectroscopy [3]. Although it is now generally accepted that the strong peak centered around 15.5 eV is due to the shape resonantly enhanced $2\sigma_u \rightarrow \pi_g$ transition, the assignment of the other prominent features is the subject of much debate and still remains uncertain. For example Ukai et al. [21] identify the transition at 13.3 eV as due to a $1\pi_u \rightarrow 4\sigma$ valence transition, while Hattori et al. [22] propose that the $3\sigma_g \rightarrow 3\sigma_u$ and $3\sigma_g \rightarrow 3p\sigma_u$ transitions are located at 13.3 and 13.8 eV, respectively. Hayaishi et al. [10] have performed ab initio calculations showing that a $3\sigma_g \rightarrow 3\sigma_u$ transition occurs at around 13.3 eV, which is broadened by a change in geometry of the excited state, with the strong intensity variations being caused by interference effects. Superimposed on these features are sharp but weak contributions from Rydberg states starting at 14.25 eV [10]. In the present work a strong feature, not seen in earlier ion yield experiments, is also observed at 17.0 eV. According to the calculations of Hattori et al. [22] this energy coincides with the $2\sigma_u \rightarrow 4s\sigma_g$ transition. However, it should be noted that they estimate an extremely small *f* value for this transition. Above 18 eV the ion yield curve is relatively smooth and shows only weak features associated with Rydberg states.

Table 1 shows the measured appearance potentials obtained from the fragment ion yield curves shown

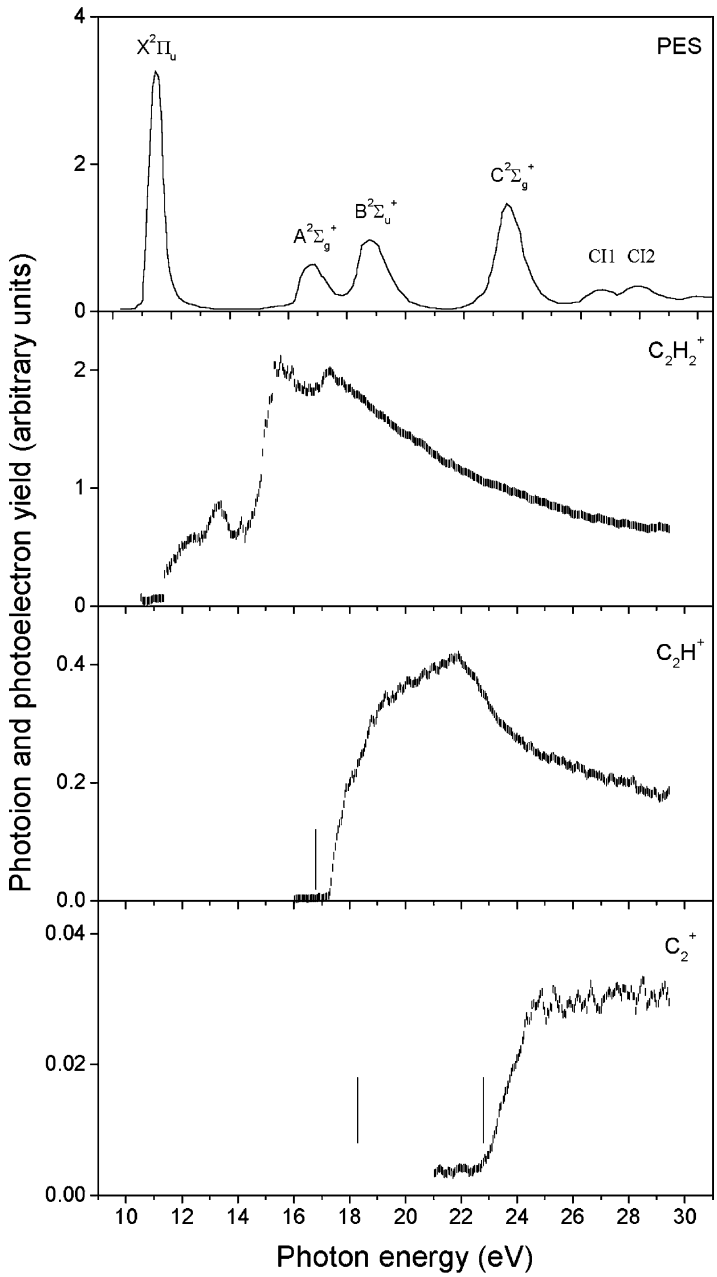

Fig. 1. Positive photoion yield curves for the indicated ion fragments from acetylene, with the photoelectron spectrum of Holland et al. [5]. Lines show thermochemical thresholds (see Table 1).

in Figs. 1 and 2. In all cases the measured thresholds are close to their thermochemical values and in general accord with the other lower resolution experimental estimates where available. Above threshold, in the case of C_2H^+, two distinct and as yet unexplained features are observed at energies of 18.1 and 18.8 eV for the first time. In the case of C^+ production, the steps at higher energies clearly correspond to

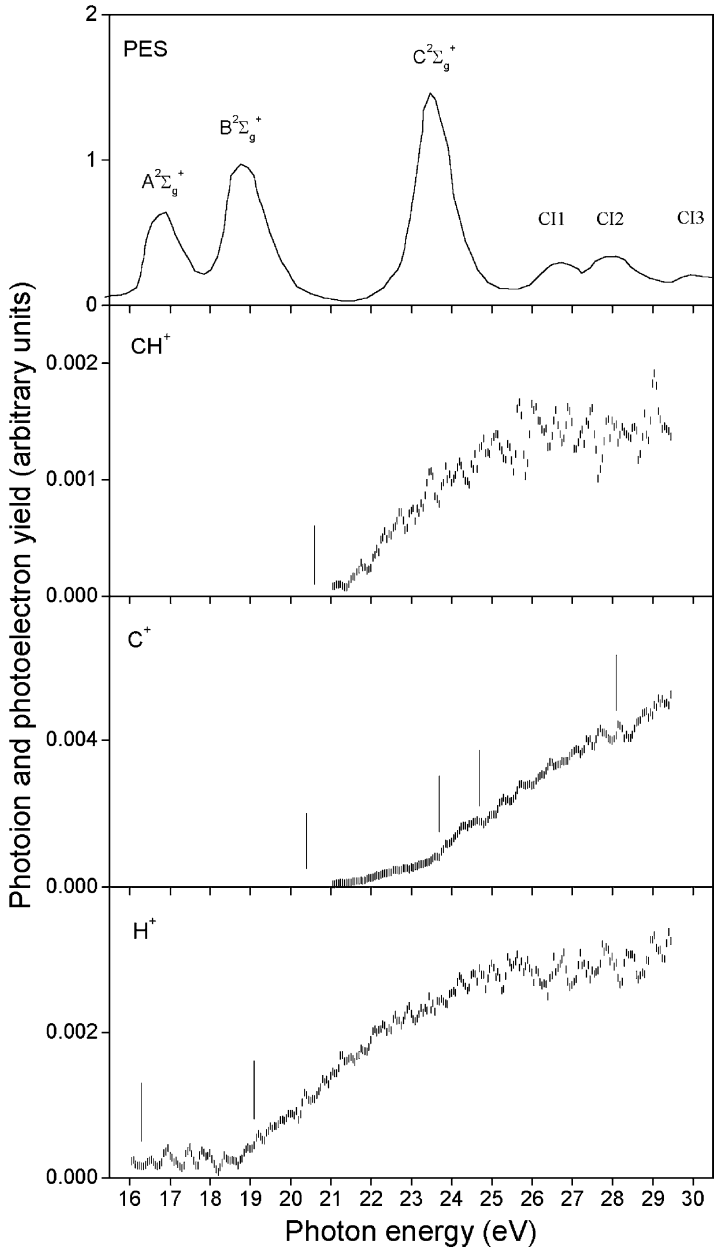

Fig. 2. Positive photoion yield curves for the indicated ion fragments from acetylene, with the photoelectron spectrum of Holland et al. [5]. Lines show thermochemical thresholds (see Table 1).

the thermochemical thresholds for the different neutral fragment channels given in Table 1. The threshold for H^+ formation (18.9 ± 0.1 eV) is significantly different from the only previous measurement (22.5 ± 1 eV) but is in harmony with the thermochemical threshold. At energies above 22 eV, all the fragment ion yield curves become relatively smooth and there are no observable effects corresponding to the satellite CI states [5].

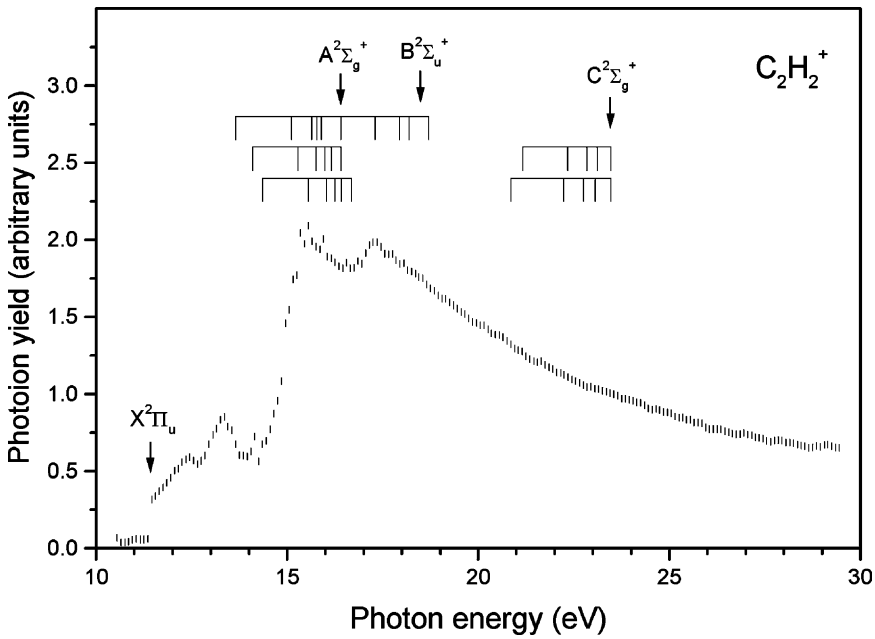

Fig. 3. Photoion yield curve for $C_2H_2^+$ from acetylene. Lines indicate calculated Rydberg series from Ibuki et al. [7] converging to the ion states [5] shown (arrows).

Fig. 4 shows the negative photoion yield curve for C_2H^- formation in C_2H_2 along with the photoabsorption spectrum of Ukai et al. [21] and the ionization thresholds obtained from photoelectron spectroscopy. Clearly, the main processes leading to ion pair formation, which necessarily arise from excited neutral states of acetylene, cannot be seen in the photoabsorption spectrum. The observed threshold for this process, at 16.30 eV, is in excellent agreement with the thermochemical calculation and observation of Ruscic

Table 1
Calculated and measured appearance potentials for the production of fragment ions from acetylene

Process	Threshold energy (eV)			
	Thermochemical[a]	This work ± 0.1	Cooper et al. [30] ± 1.0	Hayaishi et al. [10] ± 0.1
C_2H^+ (H)	16.8	17.3	16.5	16.8
C_2^+ (H_2)	18.3	<21.0	18.5	18.1
C_2^+ (2H)	22.8	22.5	23.0	22.7
CH^+ (CH)	20.6	21.4	20.0	20.7
C^+ (CH_2)	20.4	21.1		
C^+ (C, H_2)	23.7	23.7	23.0	
C^+ (CH, H)	24.7	24.8	26.0	
C^+ (C, 2H)	28.1	28.2		
H^+ (C_2H)	19.1	18.9	22.5	
C_2H^- (H^+)	16.3[b]	16.3		

Brackets show undetected neutral fragments formed in each process.
[a] Calculated by Cooper et al. [30] from [31,32] except [23].
[b] Calculated by Ruscic and Berkowitz [23].

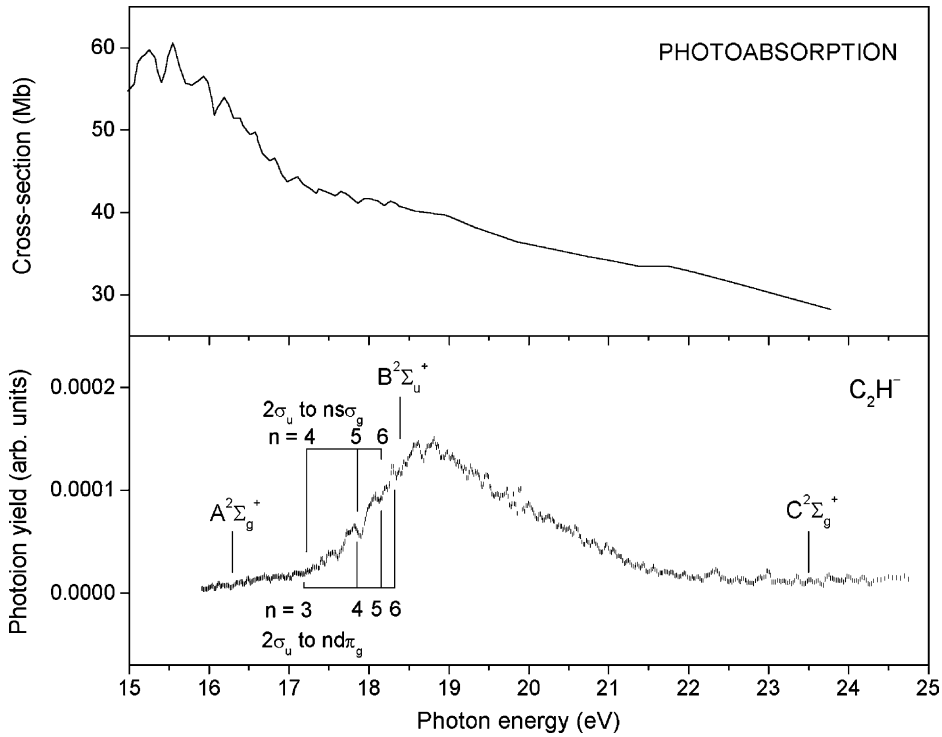

Fig. 4. Negative photoion yield curve for C_2H^- from acetylene with the photoabsorption spectrum of Ukai et al. [21]. The Rydberg series calculated by Langhoff et al. [24] and ion states [5] are also shown.

and Berkowitz [23]. This threshold, when combined with the electron affinity of C_2H (2.97 ± 0.01 eV), yields D_0(HCC–H) $= 5.70 \pm 0.02$ eV, also in agreement with the earlier work. Above threshold, the negative ion yield curve rises up to a maximum at around 18.8 eV, before slowly falling away at higher energies. The weak but sharp structure observed on the rising portion clearly correlates with the energies of predicted predissociating Rydberg states converging to the $B^2\Sigma_u^+$ state of $C_2H_2^+$ as calculated by Langhoff et al. [24]. A similar series of predissociating Rydberg states converging to the $C^2\Sigma_g^+$ state can also be seen to contribute between 21 and 24 eV. It is also noticeable that these features are superimposed on a broad ~2 eV wide band, and that no Rydberg states are predicted between 18.7 and 21.0 eV. The irregular structure observed in this energy range can be attributed to vibrational progressions of the $B^2\Sigma_u^+$ state, as identified by Avaldi et al., in their threshold photoelectron spectra [3]. The general position and overall shape of this broad band is typical of a shape resonance, which commonly has a lifetime of 10^{-14} to 10^{-15} s, corresponding to a width between 1 and 10 eV. Farren et al. [25] have performed calculations to investigate the origins and characteristics of shape resonance features in acetylene and have demonstrated the important role played by virtual valence orbitals σ^* in this energy region. In addition, the existence of such resonances in photoabsorption in acetylene above the C 1s ionization threshold has been evaluated and confirmed by Piancastelli [26]. An alternative possibility is that the broadening is due to direct Frank–Condon excitation to the repulsive portion of a pseudo-diatomic $^1\Sigma_u$ C_2H^-–H^+ ion pair state [23,26], which also predissociates via excitation to vibrationally broadened progressions of Rydberg states [3].

3.2. Ethylene

The ethylene molecule has a linear $D_{\infty h}$ geometry and the ground state configuration and term [26]

$$\underset{\text{core orbitals}}{(1a_g)^2(1b_{lu})^2} \quad \underset{\text{inner valence}}{(2a_g)^2(2b_{lu})^2}$$
$$\underset{\text{outer valence}}{(1b_{2u})^2(3a_g)^2(1b_{3g})^2(1b_{3u})^2} \quad {}^1A_g$$

with the three lowest lying virtual orbitals being ($4a_g$), ($3b_{1u}$), and ($1b_{2g}$). The outermost valence orbitals are derived primarily from the C 2p and H 2s atomic orbitals. High resolution HeI photoelectron spectroscopy has shown that the adiabatic ionization energies for $C_2H_4^+$ X^2B_{3u}, A^2B_{3g}, B^2A_g, C^2B_{2u} and D^2B_{1u} states are 10.51, 12.45, 14.45, ∼15 and 18.82 eV, respectively and that ionization is well described by the independent particle model only for the lowest three of these states [27]. At higher energies, however, experimental and theoretical studies have demonstrated that ionization from the ($2a_g$) and ($2b_{1u}$) orbitals leads to the creation of a large number of final states due to electron correlation effects.

Photoion yield curves for the parent and main fragment ions formed in C_2H_4 taken with a resolution of 10 meV are shown in Figs. 5 and 6, along with the photoelectron spectrum of Holland et al. [27] taken with HeII radiation at 40.8 eV. As in the case of the acetylene, the general features of the present data are in satisfactory accord with the earlier low resolution electron energy loss experiments [7]. The photoion yield curve for the parent $C_2H_4^+$ parent ion has an appearance potential of 10.5 eV and is in excellent accord with the value established by photoelectron spectroscopy. Between threshold and ∼16 eV, the yield curve rises steadily, with clear steps only appearing at each ionization threshold appearing in the photoelectron spectrum and, in this case, no obvious signs of effects due to autoionizing states. Above 16 eV, however, strong features due to autoionizing superexcited states, most noticeably at 16.5 and 17.3 eV where no known states exist, are seen in the region between the C and D ion states. At higher energies, no effects due to either the CI or E^2A_g states are seen and the yield curve decays smoothly.

Table 2 shows the measured appearance potentials obtained from the fragment ion yield curves shown in Figs. 5 and 6. The $C_2H_3^+$ and $C_2H_2^+$ ions clearly have thresholds associated with the A^2B_{3g} and B^2A_g states of the parent ion and are close to their thermochemical values. The statistical dissociation of $C_2H_4^+$ in accordance with QET therefore implies that these states undergo rapid electronic relaxation to the ground electronic state [7]. The remaining fragments all have thresholds associated with the D^2B_{lu} state of the parent ion and are typically 0.5–1.5 eV above the thermochemical values. Agreement with the lower resolution experimental estimates obtained by electron impact is relatively poor, especially for this latter group of ions. Above threshold the $C_2H_3^+$ curve shows distinct structure at 16.5, 17.25 and 17.7 eV. The $C_2H_2^+$ results also display the feature around 17.25 eV, as

Table 2
Calculated and measured appearance potentials for the production of fragment ions from ethylene

Process	Threshold energy (eV)		
	Thermochemical[a]	This work ± 0.1	Ibuki et al. [7] ± 1.0
$C_2H_3^+$ (H)	13.3	13.3	13.0
$C_2H_2^+$ (H_2)	13.1	13.0	12.5
C_2H^+ (H_2, H)	18.6	19.5	22.0
CH_3^+ (CH)	16.9	18.35	17.0
CH_2^+ (CH_2)	17.9	18.35	18.5
H^+ (C_2H_3)	17.5	18.35	20.5
H^- ($C_2H_3^+$)	12.55	≤13.0	

Brackets show undetected neutral fragments formed in each process.
[a] Calculated by Ibuki et al. [7] from [32].

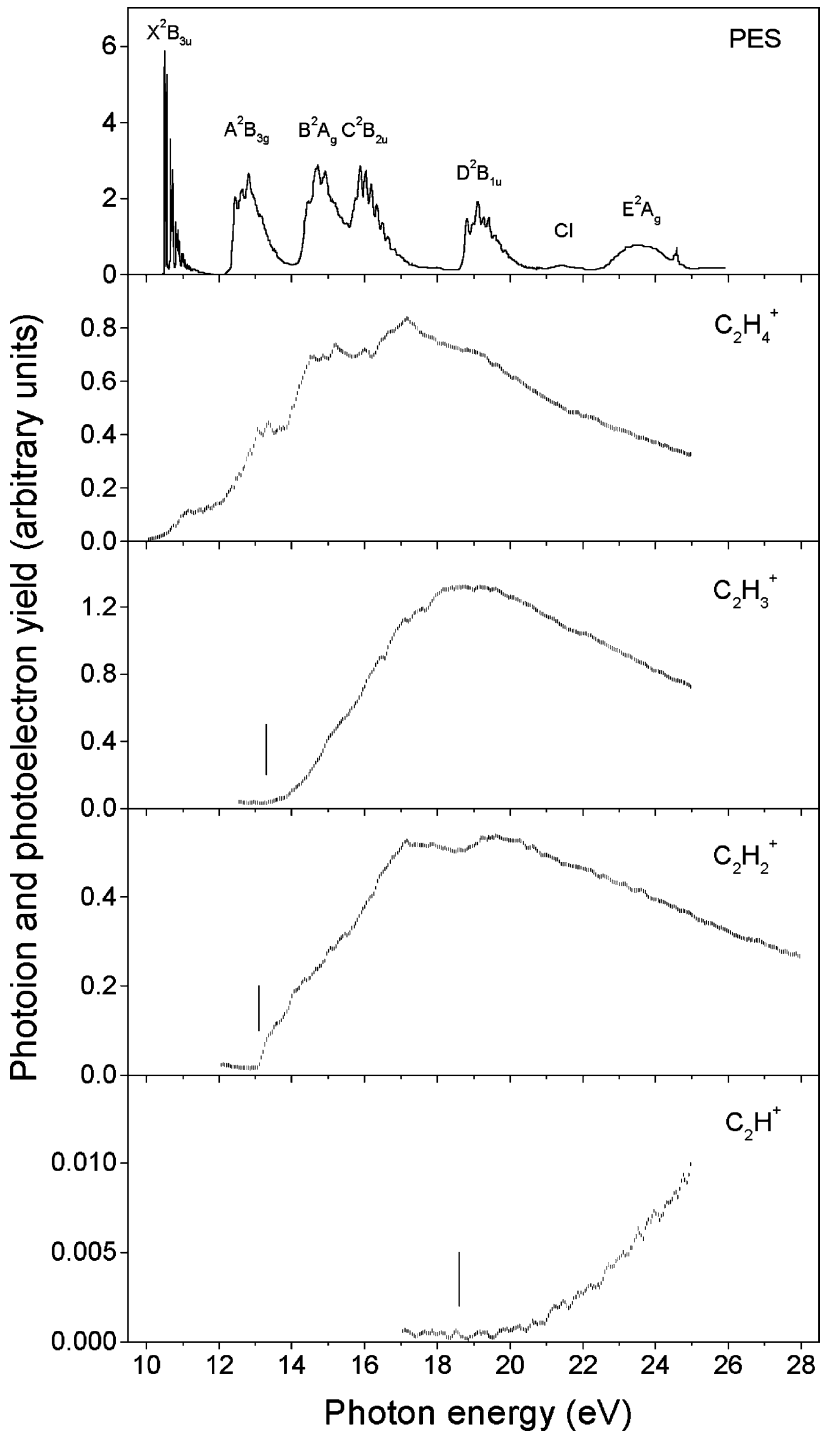

Fig. 5. Positive photoion yield curves for the indicated ion fragments from ethylene, with the photoelectron spectrum of Holland et al. [27]. Lines show thermochemical thresholds (see Table 2).

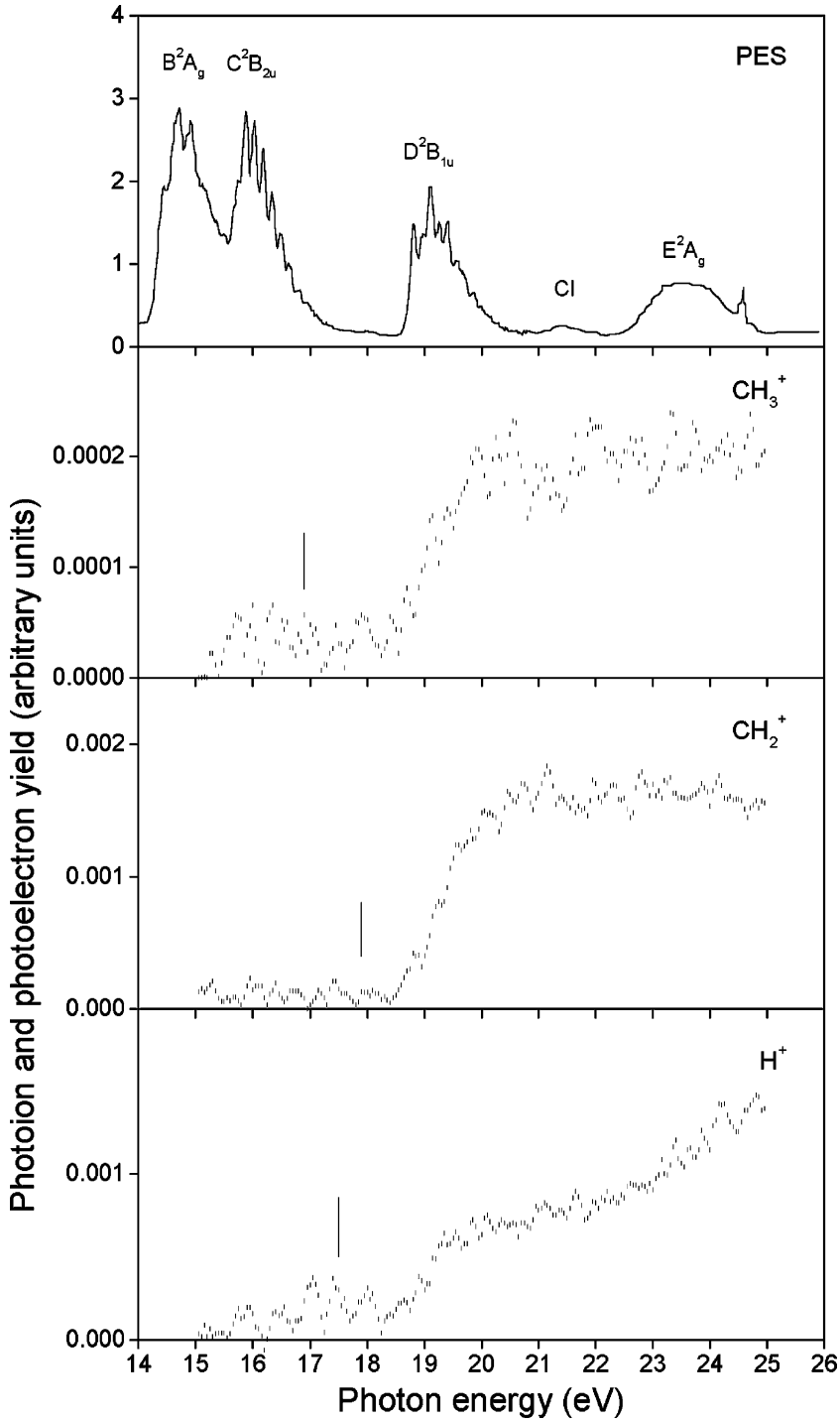

Fig. 6. Positive photoion yield curves for the indicated ion fragments from ethylene, with the photoelectron spectrum of Holland et al. [27]. Lines show thermochemical thresholds (see Table 2).

well as enhancement at the onset of the D state. The calculations of Desjardins et al. [28] predict a satellite state at 17.2 eV corresponding to an ionic state of $^2B_{2g}$ symmetry. However, many-body Green's function calculations give an energy of 17.83 eV [29] for this state. Our results do not permit any conclusions on this difference, but they do confirm the existence of several states in this energy region.

Fig. 7 shows the negative photoion yield curve for H^- formation in C_2H_4 along with the photoabsorption spectrum of Holland et al. [27]. Clearly, the main processes leading to ion pair formation, which necessarily arise from excited neutral states of ethylene can, in contrast to the situation in acetylene, be observed in the photoabsorption spectrum. In both sets of data substantial structure is observed in the energy region below 20 eV, which is shown in more detail in Fig. 8. It can be seen that the details of this structure are in accord with vibrational progressions associated with Rydberg states, as identified by Holland et al. [27], who also showed that predissociation into neutral products competes successfully with autoionization

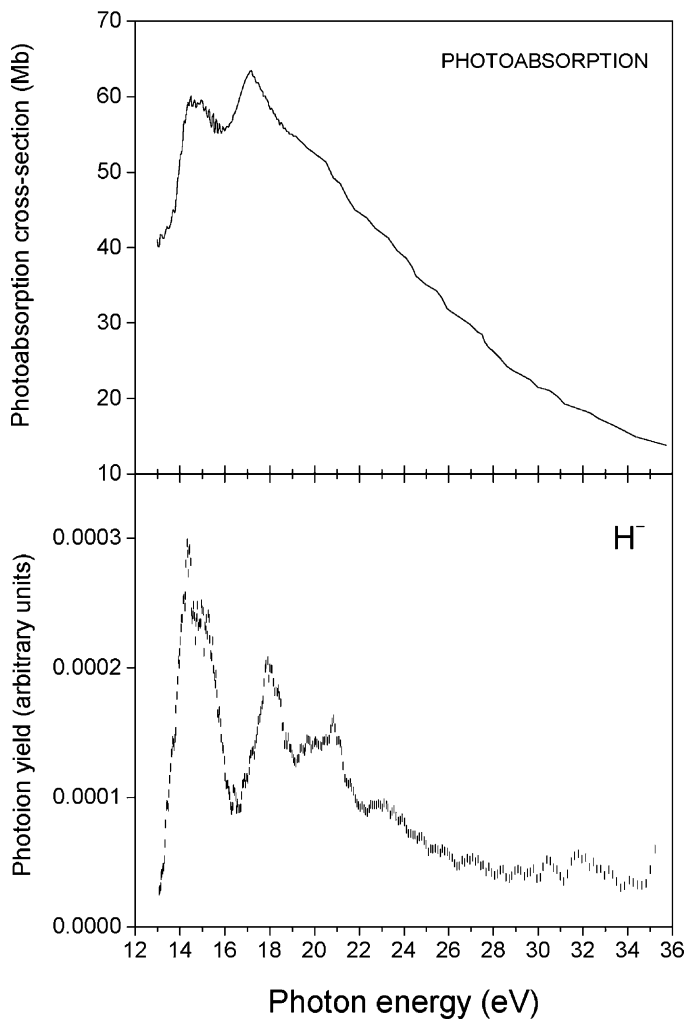

Fig. 7. Negative photoion yield curve for H^- from ethylene with the photoabsorption spectrum of Holland et al. [27].

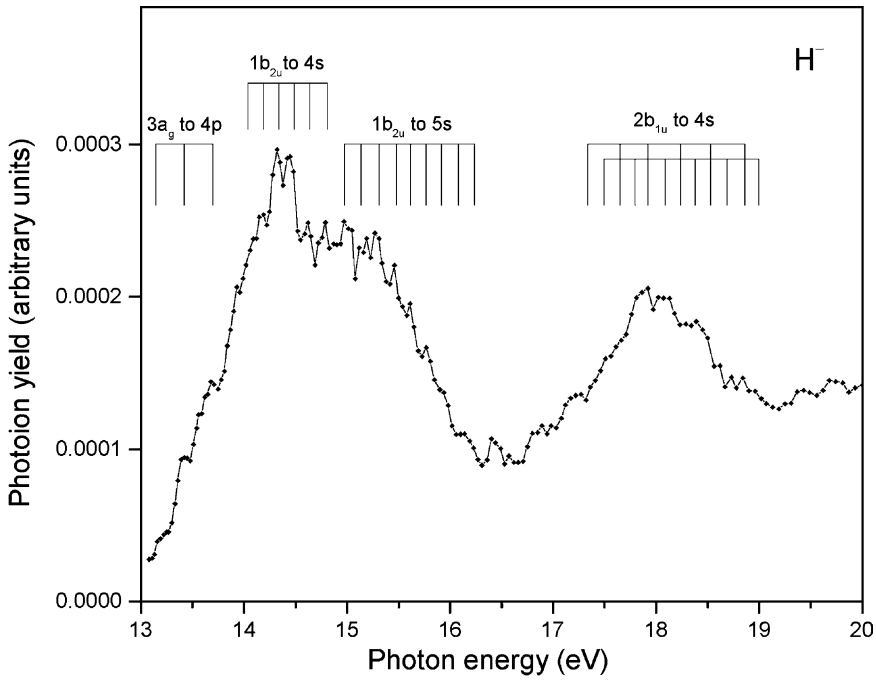

Fig. 8. Negative photoion yield curve for H^- from ethylene. Vibrational progressions of Rydberg series identified by Holland et al. [27] are also shown.

in the decay of these excited states. The present work shows that, in addition, predissociation involving ion pair formation makes a significant contribution. Additional structure, not seen in photoabsorption, is observed in the negative ion yield curve at energies above 20 eV and is undoubtedly associated with a predicted CI state at 20.45 eV and Rydberg levels approaching the $2a_g^-$ (E^2A_g) ion state [27]. However, as in the case of acetylene, the possibility that shape resonances are broadening and enhancing these inner valence negative ion spectra cannot be excluded.

Acknowledgements

The support of the UK Engineering and Physical Science Research Council in providing a research grant is gratefully acknowledged. AMS and SWJS were the recipients of ESF and Department of Education, Northern Ireland postgraduate research studentships, respectively.

References

[1] S.H. Zheng, S.K. Srivastava, J. Phys. B: Atom. Mol. Opt. Phys. 29 (1996) 3235.
[2] S.L. Lunt, J. Randell, J.P. Ziesel, G. Mrotzek, D. Field, J. Phys. B: Atom. Mol. Opt. Phys. 27 (1994) 1407.
[3] L. Avaldi, G. Dawber, R.I. Hall, G.C. King, A.G. McConkey, M.A. MacDonald, G. Stefani, J. Electron Spectrosc. Relat. Phenom. 71 (1995) 93.
[4] G. Bieri, L. Åsbrink, J. Electron Spectrosc. Relat. Phenom. 20 (1980) 149.
[5] D.M.P. Holland, M.A. MacDonald, M.A. Hayes, L. Karlsson, B. Wannberg, J. Electron Spectrosc. Relat. Phenom. 104 (1999) 245.
[6] G. Cooper, G.R. Burton, C.E. Brion, J. Electron Spectrosc. Relat. Phenom. 73 (1995) 139.
[7] T. Ibuki, G. Cooper, C.E. Brion, Chem. Phys. 129 (1989) 295.
[8] R. Botter, V.H. Dibeler, J.A. Walker, H.M. Rosenstock, J. Chem. Phys. 44 (1966) 1271.
[9] J. Berkowitz, Photoabsorption, Photoionization and Photoelectron Spectroscopy, Academic Press, New York, 1979.
[10] T. Hayaishi, S. Iwata, M. Sasanuma, E. Ishiguro, Y. Morioka, Y. Iida, M. Nakamura, J. Phys. B: Atom. Mol. Opt. Phys. 15 (1982) 79.
[11] W.A. Chupka, J. Berkowitz, K.M.A. Rafaey, J. Chem. Phys. 50 (1969) 1938.

[12] R. Stockbauer, M.G. Inghram, J. Chem. Phys. 62 (1975) 4862.
[13] K.V. Wood, J.W. Taylor, Int. J. Mass Spectrom. Ion Phys. 30 (1979) 307.
[14] J. Berkowitz, in: U. Becker, D.A. Shirley (Eds.), VUV and Soft X-ray Photoionization, Plenum Press, New York, 1996.
[15] K. Mitsuke, H. Hattori, H. Yoshida, J. Chem. Phys. 99 (1993) 6642.
[16] R.A. Mackie, A.M. Sands, S.W.J. Scully, D.M.P. Holland, D.A. Shaw, K.F. Dunn, C.J. Latimer, J. Phys. B: Atom. Mol. Opt. Phys. 35 (2002) 1061.
[17] C.J. Latimer, R.A. Mackie, A.M. Sands, N. Kouchi, K.F. Dunn, J. Phys. B: Atom. Mol. Opt. Phys. 32 (1999) 2667.
[18] J.A.R. Samson, R.B. Cairns, Rev. Sci. Inst. 36 (1965) 19.
[19] R. Browning, H.B. Gilbody, J. Phys. B: Atom. Mol. Opt. Phys. 1 (1968) 1149.
[20] J.E. Reutt, L.S. Wang, J.E. Pollard, D.J. Trevor, Y.T. Lee, D.A. Shirley, J. Chem. Phys. 34 (1986) 3022.
[21] M. Ukai, K. Kameta, R. Chiba, K. Nagano, N. Kouchi, K. Shinsaka, Y. Hatano, H. Umemoto, Y. Ito, K. Tanaka, J. Chem. Phys. 95 (1991) 4142.
[22] H. Hattori, Y. Hikosaka, T. Hikida, K. Mitsuke, J. Chem. Phys. 106 (1997) 4902.
[23] B. Ruscic, J. Berkowitz, J. Chem. Phys. 93 (1990) 5586.
[24] P.W. Langhoff, B.V. McKoy, R. Unwin, A.M. Bradshaw, Chem. Phys. Lett. 83 (1981) 270.
[25] R.E. Farren, J.A. Sheehy, P.W. Langhoff, Chem. Phys. Lett. 177 (1991) 307.
[26] M.N. Piancastelli, J. Electron Spectrosc. Relat. Phenom. 100 (1999) 167.
[27] D.M.P. Holland, D.A. Shaw, M.A. Hayes, L.G. Shpinkova, E.E. Rennie, L. Karlsson, P. Baltzer, B. Wannberg, Chem. Phys. 219 (1997) 91.
[28] S.J. Desjardins, A.D.O. Bawagan, Z.F. Liu, K.H. Tan, Y. Wang, E.R. Davidson, J. Chem. Phys. 102 (1995) 6385.
[29] L.S. Cederbaum, W. Domcke, J. Schirmer, W. von Niessen, G.H.F. Diercksen, W.P. Kraemer, J. Chem. Phys. 69 (1978) 1591.
[30] G. Cooper, T. Ibuki, Y. Iida, C.E. Brion, Chem. Phys. 125 (1988) 307.
[31] Y. Ono, C.Y. Ng, J. Chem. Phys. 74 (1981) 6985.
[32] H.M. Rosenstock, K. Draxl, B.W. Steiner, J.T. Herron, J. Phys. Chem. Ref. Data 6 (Suppl. 1) (1977) 1.